Front. Phys. 13(3), 137801 (2018)
https://doi.org/10.1007/s11467-018-0746-6

RESEARCH ARTICLE

Fano resonances in heterogeneous dimers of silicon and gold nanospheres

Qian Zhao, Zhong-Jian Yang†, Jun He

Hunan Key Laboratory of Super Microstructure and Ultrafast Process, School of Physics and Electronics, Central South University, Changsha 410083, China
Corresponding author. E-mail: †zjyang@csu.edu.cn
Received October 26, 2017; accepted December 5, 2017

We theoretically investigate the optical properties of dimers consisting of a gold nanosphere and a silicon nanosphere. The absorption spectrum of the gold sphere in the dimer can be significantly altered and exhibits a pronounced Fano profile. Analytical Mie theory and numerical simulations show that the Fano profile is induced by constructive and destructive interference between the incident electric field and the electric field of the magnetic dipole mode of the silicon sphere in a narrow wavelength range. The effects of the silicon sphere size, distance between the two spheres, and excitation configuration on the optical responses of the dimers are studied. Our study reveals the coherent feature of the electric fields of magnetic dipole modes in dielectric nanostructures and the strong interactions of the coherent fields with other nanophotonic structures.

Keywords silicon nanosphere, gold nanosphere, magnetic dipole resonance, Fano resonance, Mie theory

PACS numbers 78.67.-n, 42.25.Kb, 42.25.Hz

1 Introduction

Dielectric nanostructures have recently attracted considerable interest, as they exhibit strong optical responses, and their material losses are low [1–3]. The strong optical responses typically arise from different magnetic and electric modes, which are leaky geometrical resonances. These optical properties make dielectric nanostructures attractive for many photonic applications such as optical antennas [4, 5], metasurfaces or metamaterials [6–8], solar cells [9], and structural colors [10]. The building blocks for these applications are typically simple dielectric nanoresonators with different geometric shapes, such as spherical particles [11, 12], cylinders or disks [13, 14], and nanoblocks [15]. Complete understanding of the optical responses of these simple resonators is essential for better realizing the above photonic functionalities.

The optical properties of individual simple nanoresonators have been extensively investigated [11–15]. Low-order electric and magnetic resonances can be readily excited in these structures, for example, the electric dipole (ED) and magnetic dipole (MD) modes. Many optical phenomena involving interaction of the electric and/or magnetic resonant modes in dielectric nanostructures have been demonstrated, such as magnetic near-field enhancement [16, 17], directional scattering [18, 19], and Fano resonances [20–24]. The couplings between the optical responses of dielectric nanostructures and the surface plasmon resonances of metal nanostructures have also been investigated, and directional scattering [25–27] and Fano resonances [28, 29] have been observed. Fano resonances in photonic nanostructures usually involve constructive and destructive interference between broad and narrow spectral responses [30].

In this work, we theoretically investigate the optical properties of dimers consisting of a gold (Au) nanosphere and a silicon (Si) nanosphere. The ED and MD modes of the Si sphere are spectrally covered by the Au interband transitions. In such a dimer, the absorption spectrum of the Au sphere is changed greatly and exhibits a Fano profile in which the plane wave propagates from one sphere to the other. Analytical Mie theory and numerical simulations show that the magnetic dipole polarizability varies dramatically from a negative minimum value to a positive maximum value in a narrow wavelength range around the MD mode of the Si sphere. This variation causes constructive and destructive interference between

the incident electric field and the electric field of the MD mode, and induces the Fano profile in the Au absorption spectrum. The effects of the size of the silicon spheres and the distance between the two spheres on the Fano resonances are studied. The optical responses of dimers with different excitation configurations are also considered. Our study reveals the coherent properties of the electric field associated with the MD modes in dielectric nanostructures and the strong modifications of the optical responses of other nanophotonic structures nearby. These features may find applications in composite nanophotonic devices including photon–exciton hybrid nanostructures [31, 32].

2 Results and discussion

Figure 1(a) shows a schematic of a dimer system with a plane wave as the excitation source. The optical responses are calculated using commercial finite-difference time-domain (FDTD) software (Lumerical FDTD). The dielectric constants of Si and Au are taken from Palik's book [33]. Figure 1(b) shows the scattering and absorption spectra of individual Au and Si spheres. The radii of the Au and Si spheres are 40 and 50 nm, respectively. For the Au sphere, the absorption cross section is much larger than the scattering cross section. There is an electric dipole plasmon resonance near $\lambda = 510$ nm. The interband transitions in the Au material contribute to the responses below $\lambda \approx 500$ nm. There are two main peaks in the spectra of the Si sphere. They correspond to an ED resonance ($\lambda \approx 400$ nm) and an MD resonance ($\lambda \approx 465$ nm).

Figure 1(c) shows the optical responses of a coupled dimer, where the wave vector is along the $-x$ direction. The ED and MD resonance lineshapes of the Si sphere are weakly affected in the dimer. However, the absorption spectrum of the Au sphere is greatly modified, and an obvious Fano-like profile can be observed around the MD resonant wavelength of the Si sphere. When the wave vector of the light is along the $+x$ direction [Fig. 1(d)], the Au sphere also shows a Fano-like response similar to that in Fig. 1(c). Note that the absorption spectrum of the entire dimer barely shows a Fano-like feature, as

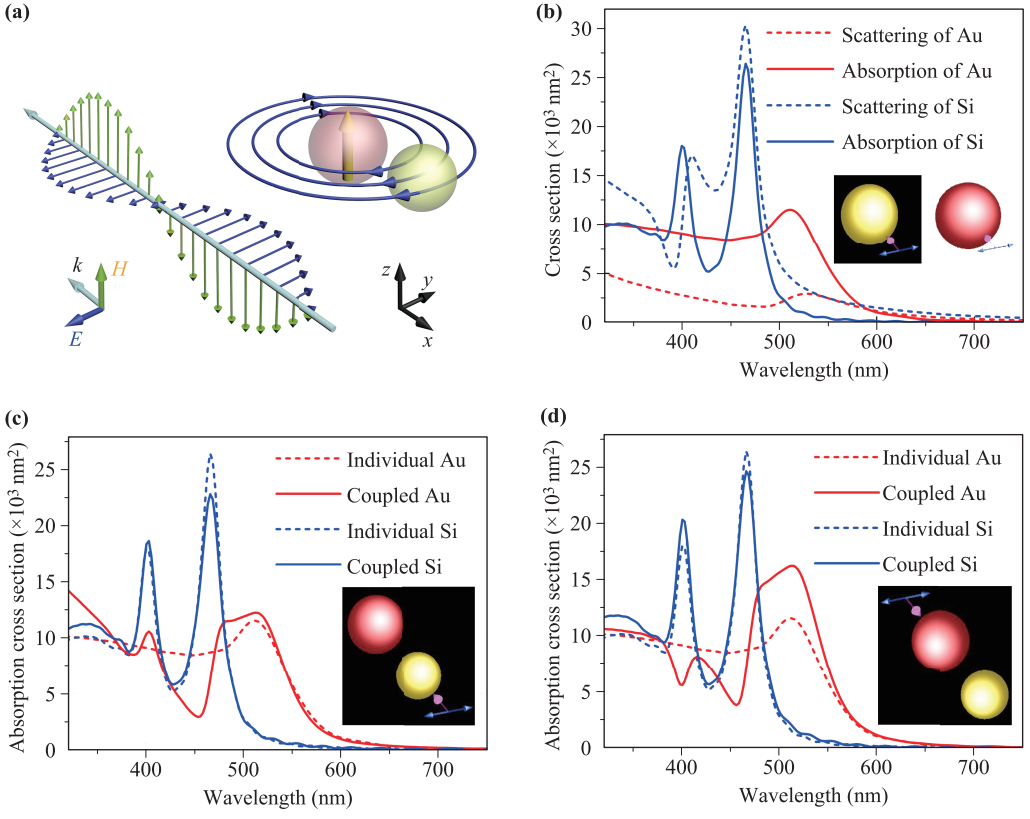

Fig. 1 **(a)** Schematic of a coupled system. The origin of the coordinates is chosen as the center of the Si sphere. **(b)** Scattering and absorption cross section spectra of individual Au and Si spheres. The radii of the Au and Si spheres are 40 and 50 nm, respectively. **(c, d)** Absorption cross section spectra of Au and Si spheres in the coupled structure. The surface distance is 10 nm. The results for individual spheres are also shown for comparison. The wave vectors of the plane waves in (c) and (d) are in the $-x$ and $+x$ directions, respectively.

it is dominated by the Si sphere, and the absorption of the Si sphere is modified slightly in the dimer. The interband transitions of the Au sphere can be excited by both the electric field associated with the light source and the MD mode of the Si sphere. Thus, understanding the relative phase between the incident field and the field scattered by the Si sphere is important to explain the above Fano-like resonances. We will use the Mie scattering theory to describe the optical responses of an individual Si nanosphere.

Consider a Si nanosphere with a radius R and complex refractive index $m = n_1 + \mathrm{i}n_2$ placed in vacuum. The excitation light is a plane wave with wavelength λ and wave vector $k = 2\pi/\lambda$. Owing to the small size of the sphere ($R \sim 50$ nm) compared to the wavelength λ ($kR \ll \lambda$), the resonant modes are dominated by the ED and MD modes within the visible wavelength range. The electric and magnetic dipole moments can be written as $\boldsymbol{p} = \varepsilon_0\varepsilon_\mathrm{s}\boldsymbol{\alpha}_\mathrm{E}\boldsymbol{E}$ and $\boldsymbol{m} = (\mu_0\mu_\mathrm{s})^{-1}\boldsymbol{\alpha}_\mathrm{M}\boldsymbol{B}$, where $\varepsilon_0(\varepsilon_\mathrm{s})$ and $\mu_0(\mu_\mathrm{s})$ are the permittivity and permeability of vacuum (the sphere), respectively. Further, $\boldsymbol{\alpha}_\mathrm{E}$ and $\boldsymbol{\alpha}_\mathrm{M}$ are the electric and magnetic polarizabilities of the sphere, respectively. $\boldsymbol{E}$ and $\boldsymbol{B}$ are the external excitation fields. The polarizabilities can be rewritten as [34, 35]

$$\alpha_\mathrm{E} = \frac{\alpha_\mathrm{E}^{(0)}}{1 - \mathrm{i}\frac{k^3}{\pi^3}\alpha_\mathrm{E}^{(0)}}, \quad \alpha_\mathrm{M} = \frac{\alpha_\mathrm{M}^{(0)}}{1 - \mathrm{i}\frac{k^3}{\pi^3}\alpha_\mathrm{M}^{(0)}}, \tag{1}$$

where

$$\alpha_\mathrm{E}^{(0)} = -\frac{6\pi}{k^3}\tan\alpha_1, \quad \text{and} \quad \alpha_\mathrm{M}^{(0)} = -\frac{6\pi}{k^3}\tan\beta_1. \tag{2}$$

Further, α_1 are β_1 the scattering phase shifts satisfying

$$\begin{aligned}\tan\alpha_n &= -\frac{m^2 j_n(y)[xj_n(x)]' - j_n(x)[yj_n(y)]'}{m^2 j_n(y)[xy_n(x)]' - y_n(x)[yj_n(y)]'},\\ \tan\beta_n &= -\frac{j_n(y)[xj_n(x)]' - j_n(x)[yj_n(y)]'}{j_n(y)[xy_n(x)]' - y_n(x)[yj_n(y)]'},\end{aligned} \tag{3}$$

where $x = kR = 2\pi R/\lambda$, and $y = mx \cdot j_n(x)$ and $y_n(x)$ are the spherical Bessel and Neumann functions, respectively. The extinction and scattering cross sections can be written in terms of $\boldsymbol{\alpha}_\mathrm{M}$ and $\boldsymbol{\alpha}_E$ as $\sigma_\mathrm{ext} = k\mathrm{Im}(\boldsymbol{\alpha}_\mathrm{M} + \boldsymbol{\alpha}_\mathrm{E})$ and $\sigma_\mathrm{S} = k^4(|\boldsymbol{\alpha}_\mathrm{M}|^2 + |\boldsymbol{\alpha}_\mathrm{E}|^2)/(6\pi)$, respectively. The cross sections calculated using these formulas agree well with those calculated directly by the FDTD method (data not shown). Thus, Eqs. (1)–(3) in the limit of $x \ll 1$ are good approximations for our system. Note that the Rayleigh limit ($y \equiv m2\pi R/\lambda \ll 1$) cannot be satisfied by our system. The cross sections calculated using the Rayleigh limit, where $\alpha_\mathrm{E}^{(0)}|_{y\ll1} \approx 4\pi R^3(m^2 - 1)/(m^2 + 2)$, $\alpha_\mathrm{M}^{(0)}|_{y\ll1} \approx 4\pi R^3(m^2 - 1)k^2R^2/30$, show poor agreement with the FDTD results. Thus, we will use Eqs. (1)–(3) to study the optical properties of a Si nanosphere analytically.

Figure 2(a) shows the magnetic dipole polarizability $\boldsymbol{\alpha}_\mathrm{M}$ of a Si sphere ($R = 50$ nm) calculated by Eqs. (1)–(3). $\mathrm{Re}(\boldsymbol{\alpha}_\mathrm{M})$ shows an antisymmetric shape around $\mathrm{Re}(\boldsymbol{\alpha}_\mathrm{M}) = 0$, and the $\mathrm{Re}(\boldsymbol{\alpha}_\mathrm{M}) = 0$ point corresponds to the MD resonance peak. $\mathrm{Im}(\boldsymbol{\alpha}_\mathrm{M})$ shows a symmetric lineshape near the dipole resonance peak with positive values [$\mathrm{Im}(\boldsymbol{\alpha}_\mathrm{M}) > 0$]. The results in Fig. 2(a) indicate that the Fano-like responses of the Au sphere in Fig. 1 could result from the dramatic variation of $\mathrm{Re}(\boldsymbol{\alpha}_\mathrm{M})$ around the MD resonance of the Si sphere.

Let us investigate the responses at $\lambda_1 = 455$ nm, where $\mathrm{Re}(\boldsymbol{\alpha}_\mathrm{E})$ reaches a negative minimum value. The angle of polarizability is approximated as π for simplicity. Plane-wave light is coming from right to left ($-x$ direction) with the electric field along the y axis. The magnetic dipole moment and the corresponding magnetic field are in phase. The phase of the rotating electric field associated with a MD has a $\pi/2$ delay compared to the dipole moment of the MD ($\int_L \boldsymbol{E}\mathrm{d}l = -\mathrm{d}\int_S \boldsymbol{B}\mathrm{d}\boldsymbol{S}/\mathrm{d}t$). Therefore, when the plane wave has a maximum electric field in the $-y$ direction at $x = -\lambda_1/4 \approx -111$ nm, which has a $\pi/2$ spatial phase difference from the center of Si sphere at $x = 0$, the induced rotating electric field associated with the MD resonance reaches the maximum value in the clockwise direction. As a result, destructive interference occurs between the incident electric field and the induced electric field of the Si sphere around both $x = -\lambda_1/4$ and $x = \lambda_1/4$. Our direct FDTD calculations, as shown in Figs. 2(c)–(e), agree well with the above analysis based on analytical Mie theory [Fig. 2(a)]. For the Si sphere with positive polarizabilities [$\mathrm{Re}(\boldsymbol{\alpha}_\mathrm{M}) > 0$], the discussion is similar to that for $\mathrm{Re}(\boldsymbol{\alpha}_\mathrm{M}) < 0$. Take the wavelength $\lambda_2 = 480$ nm, for example. We now have constructive interference around both $x = -\lambda_2/4$ and $x = \lambda_2/4$. Direct FDTD calculations also support this analysis [Fig. 2(f)]. The Au sphere is placed 100 nm from the Si sphere in Figs. 1(c) and (d), where this distance is nearly one-fourth of the magnetic dipole resonance ($\approx \lambda_1/4, \lambda_2/4$). Thus, we obtain constructive and destructive interference between the excitation light and the light scattered by the Si sphere in a narrow wavelength range, which induces a Fano profile in the absorption spectrum of a nearby Au nanosphere (along the propagation direction of the light).

Figure 2(b) shows the electric dipole polarizability $\boldsymbol{\alpha}_\mathrm{E}$ of the same Si sphere calculated by Eqs. (1)–(3). Both $\mathrm{Re}(\boldsymbol{\alpha}_\mathrm{E})$ and $\mathrm{Im}(\boldsymbol{\alpha}_\mathrm{E})$ are positive, and the angle θ_E of the polarizability is between 0 and $\pi/2$. In this θ_E range, Fano resonance between the excitation light and the light scattered by the Si nanosphere cannot occur. Thus, a Fano profile is not observed in the Au spectra near the ED resonance ($\lambda_3 \approx 400$ nm) of the Si sphere [Figs. 1(c) and (d)]. This polarizability behavior differs from that of plasmonic nanoparticles, where the real part of the po-

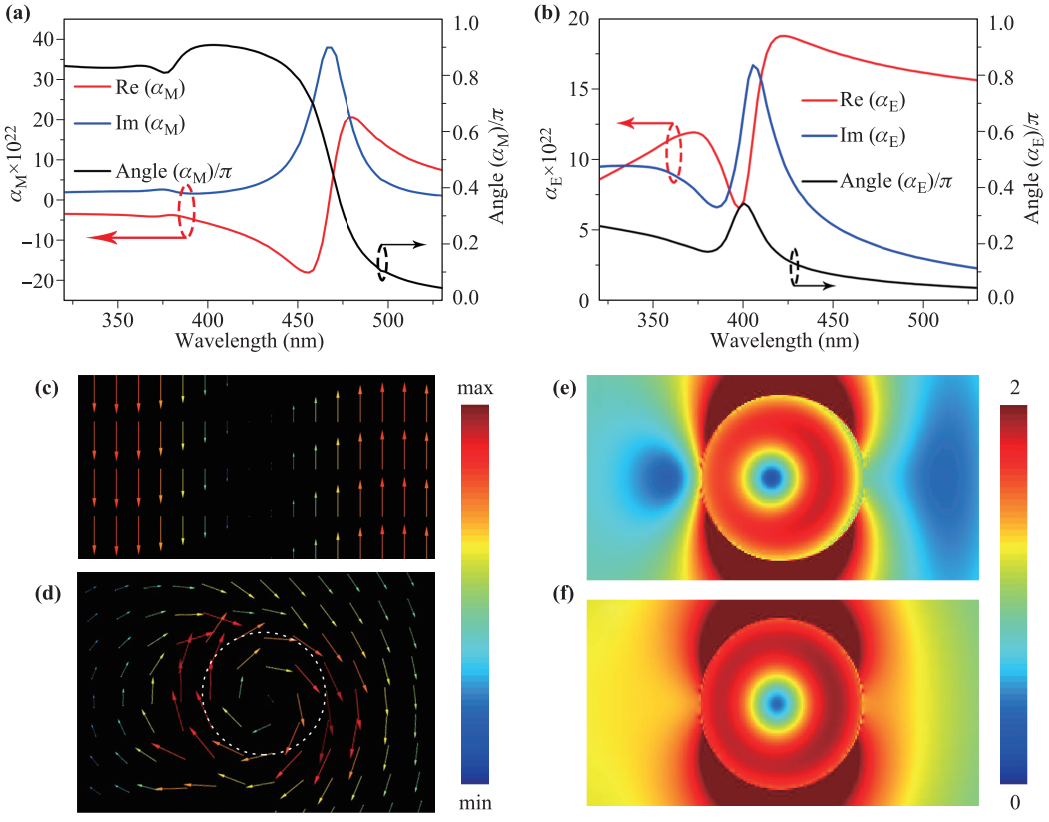

Fig. 2 Polarizability and near-field properties of a Si sphere of radius 50 nm in vacuum. **(a)** Magnetic electric polarizability $\boldsymbol{\alpha}_M$ and **(b)** electric polarizability $\boldsymbol{\alpha}_E$ of the Si sphere. The corresponding angles of the polarizabilities are also shown. **(c)** Simulated electric field vector of a light source at $\lambda_1 = 455$ nm. **(d)** Simulated scattered electric field vector of the Si sphere at $\lambda_1 = 455$ nm. The white dashed line denotes the Si sphere. **(e)** Simulated total electric field enhancement of the Si sphere at $\lambda_1 = 455$ nm. **(f)** Simulated total electric field enhancement of the Si sphere at $\lambda_2 = 480$ nm.

larizability can vary from positive to negative values [36]. Near the ED resonance ($\lambda_3 \approx 400$ nm), the Au sphere shows different absorption behavior under the two types of excitation [Figs. 1(c) and (d)]. This difference can be explained by the polarizability properties in Fig. 2(b). The phase delay between the electric dipole moment and the excitation light is θ_E, and the spatial phase difference between the two spheres is $\pi/2(\lambda_3/4)$. The electric field generated by an ED of the Si sphere is opposite to the electric dipole moment (π phase delay). Thus, for the configuration shown in Fig. 1(d), the induced electric field from the Si sphere has a phase delay of $(\theta_E - \pi/2 + \pi)$ at the position of the Au sphere. This phase difference corresponds to destructive inference between the incident field and the induced field of the Si sphere. Thus, the Au absorption is reduced when the Si sphere is present. For the configuration in Fig. 1(c), the discussion is the same as the above, but constructive inference between the incident field and the induced field of the Si sphere can be obtained. The Au absorption is increased when the Si sphere is present.

The Fano resonance of the Au sphere is tunable by shifting the MD mode of the Si sphere. Figure 3(a) shows the absorption spectra of individual Si spheres of different sizes. Both the MD and ED modes show redshifts with increasing radius. The corresponding absorption spectra of a Au sphere in the dimers with the above Si spheres are shown in Fig. 3(b). The excitation plane wave is propagating from the Si sphere to the Au sphere. The surface distance between the two spheres is fixed at 10 nm. The position of the Fano resonance closely follows the MD mode of the Si sphere and is obviously redshifted with increasing size of the Si sphere. In contrast to the Si sphere size, the distance between the two spheres has little effect on the Fano resonances of the system. We calculated dimers with surface distances of 0 to 30 nm, where the other parameters were the same as those in Figs. 1(c) and (d). The absorption spectrum of the Au sphere changed little when the distance was adjusted from 0 to 30 nm (data not shown).

The optical responses of the dimers under different excitation configurations are also investigated (Fig. 4). Figure 4(a) shows the absorption spectra of the dimer with the polarization of the incident light along the x

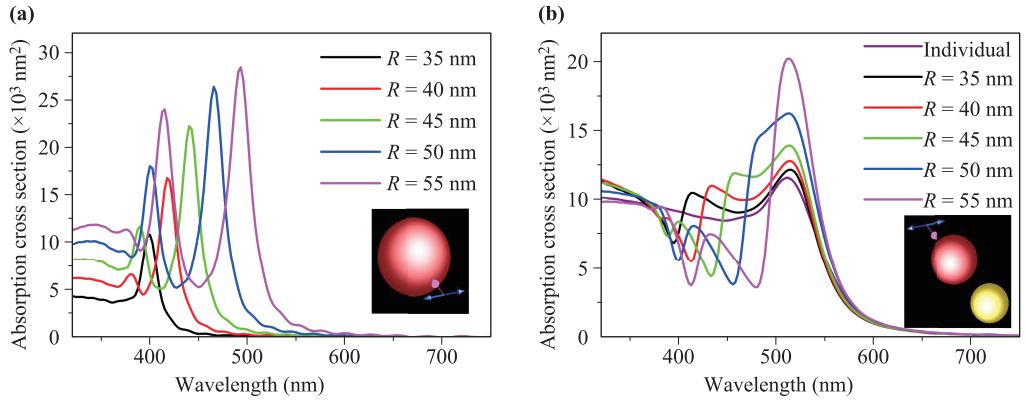

Fig. 3 **(a)** Absorption cross section spectra of individual Si spheres with radii varying from 35 to 55 nm. **(b)** Absorption cross section spectra of Au sphere in dimer structures. The radius of the Au sphere is 40 nm. The radius of the Si sphere varies from 35 to 55 nm. The wave vector of the excitation light is along the $+x$ direction, as shown in the insets.

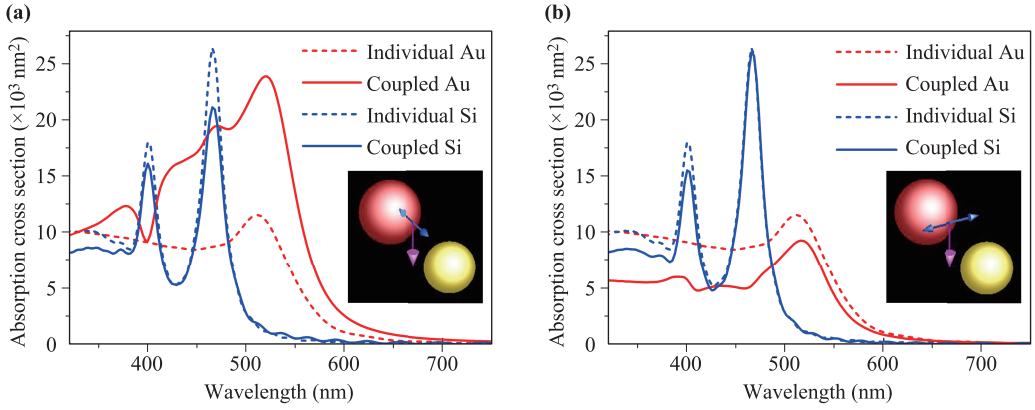

Fig. 4 Absorption spectra of Au and Si spheres in dimers with different excitation configurations. The geometries are the same as that in Fig. 1. **(a)** Polarization of the incident light is along the x axis. **(b)** Polarization and wave vector of the incident light are along the z and y axes, respectively.

axis. The absorption spectrum of the Au sphere does not exhibit Fano resonance, but its magnitude is greatly enhanced in a broad wavelength range. This enhancement is caused by both the ED and MD resonances of the Si sphere. For the MD resonance, the induced electric field is perpendicular to the excitation field near the Au sphere. For the ED resonance, the induced electric field is in phase with the excitation field near the Au sphere. Thus, the total field is always larger than the excitation field in a broad range. Figure 4(b) shows the case where the polarization and wave vector of the incident light are along the z and y axes, respectively. The absorption spectrum of the Au sphere does not exhibit Fano resonance, and its magnitude becomes smaller. Near the MD mode, the total field enhancement near the center of the rotating electric field of the MD mode is lower than the excitation field. The electric field of the ED mode undergoes destructive interference with the incident field [Fig. 2(b)]. Thus, the total electric field is lower than the excitation field in a broad range.

3 Conclusions

In conclusion, a Fano profile has been found in the absorption spectrum of a Au nanosphere in a dimer consisting of a Au nanosphere and a Si nanosphere, where the excitation plane wave propagates from the Au sphere to the Si sphere, or in the opposite direction. We conducted both Mie theory analysis and numerical simulations, and found that the Fano profiles are induced by constructive and destructive interference between the excitation electric field and the induced electric field of the MD mode of the Si sphere in a narrow wavelength range. The ED mode of the Si sphere cannot induce Fano resonance in the absorption spectrum of the Au sphere in this dimer. As the size of the Si sphere increases, the Fano resonance is redshifted because the MD mode of the Si sphere is redshifted. The Fano resonance is affected only slightly by the distance between the nanospheres (0–30 nm). The optical responses of dimers with other

excitation configurations (polarization and propagation directions) were discussed in addition, where Fano resonance has not been observed. It is difficult to directly measure the absorption spectrum experimentally; furthermore, the Au sphere is only part of the dimer. However, the Fano feature of the electric field interference should be verified by photoemission electron microscopy or near-field scanning optical microscopy. Our study reveals the coherent spatial and spectral properties of the electric field associated with the MD modes in dielectric nanostructures and their strong interactions with other nanophotonic structures nearby. These properties may find applications in composite nanophotonic devices.

Acknowledgements This work was supported by the National Natural Science Foundation of China (Grant No. 11704416) and the Hunan Provincial Natural Science Foundation of China (Grant No. 2017JJ3408).

References

1. A. I. Kuznetsov, A. E. Miroshnichenko, M. L. Brongersma, Y. S. Kivshar, and B. Luk'yanchuk, Optically resonant dielectric nanostructures, *Science* 354(6314), aag2472 (2016)
2. Z. J. Yang, R. Jiang, X. Zhuo, Y. M. Xie, J. Wang, and H. Q. Lin, Dielectric nanoresonators for light manipulation, *Phys. Rep.* 701, 1 (2017)
3. I. Staude and J. Schilling, Metamaterial-inspired silicon nanophotonics, *Nat. Photonics* 11(5), 274 (2017)
4. M. Caldarola, P. Albella, E. Cortes, M. Rahmani, T. Roschuk, G. Grinblat, R. F. Oulton, A. V. Bragas, and S. A. Maier, Non-plasmonic nanoantennas for surface enhanced spectroscopies with ultra-low heat conversion, *Nat. Commun.* 6, 7915 (2015)
5. A. E. Krasnok, A. E. Miroshnichenko, P. A. Belov, and Y. S. Kivshar, All-dielectric optical nanoantennas, *Opt. Express* 20(18), 20599 (2012)
6. D. Lin, P. Fan, E. Hasman, and M. L. Brongersma, Dielectric gradient metasurface optical elements, *Science* 345(6194), 298 (2014)
7. M. Khorasaninejad, W. T. Chen, R. C. Devlin, J. Oh, A. Y. Zhu, and F. Capasso, Metalenses at visible wavelengths: Diffraction-limited focusing and subwavelength resolution imaging, *Science* 352(6290), 1190 (2016)
8. S. Jahani and Z. Jacob, All-dielectric metamaterials, *Nat. Nanotechnol.* 11(1), 23 (2016)
9. M. L. Brongersma, Y. Cui, and S. Fan, Light management for photovoltaics using high-index nanostructures, *Nat. Mater.* 13(5), 451 (2014)
10. X. Zhu, W. Yan, U. Levy, N. A. Mortensen, and A. Kristensen, Resonant laser printing of structural colors on high-index dielectric metasurfaces, *Sci. Adv.* 3(5), e1602487 (2017)
11. A. I. Kuznetsov, A. E. Miroshnichenko, Y. H. Fu, J. Zhang, and B. Luk'yanchuk, Magnetic light, *Sci. Rep.* 2(1), 492 (2012)
12. A. B. Evlyukhin, S. M. Novikov, U. Zywietz, R. L. Eriksen, C. Reinhardt, S. I. Bozhevolnyi, and B. N. Chichkov, Demonstration of magnetic dipole resonances of dielectric nanospheres in the visible region, *Nano Lett.* 12(7), 3749 (2012)
13. T. G. Habteyes, I. Staude, K. E. Chong, J. Dominguez, M. Decker, A. Miroshnichenko, Y. Kivshar, and I. Brener, Near-field mapping of optical modes on all-dielectric silicon nanodisks, *ACS Photon.* 1, 794 (2014)
14. W. Liu, J. Zhang, B. Lei, H. Hu, and A. E. Miroshnichenko, Invisible nanowires with interfering electric and toroidal dipoles, *Opt. Lett.* 40(10), 2293 (2015)
15. H. S. Ee, J. H. Kang, M. L. Brongersma, and M. K. Seo, Shape-dependent light scattering properties of subwavelength silicon nanoblocks, *Nano Lett.* 15(3), 1759 (2015)
16. R. M. Bakker, D. Permyakov, Y. F. Yu, D. Markovich, R. Paniagua-Dominguez, L. Gonzaga, A. Samusev, Y. Kivshar, B. Luk'yanchuk, and A. I. Kuznetsov, Magnetic and electric hotspots with silicon nanodimers, *Nano Lett.* 15(3), 2137 (2015)
17. Z. J. Yang, Q. Zhao, and J. He, Boosting magnetic field enhancement with radiative couplings of magnetic modes in dielectric nanostructures, *Opt. Express* 25(14), 15927 (2017)
18. J. Yan, P. Liu, Z. Lin, H. Wang, H. Chen, C. Wang, and G. Yang, Directional Fano resonance in a silicon nanosphere dimer, *ACS Nano* 9(3), 2968 (2015)
19. T. Shibanuma, P. Albella, and S. A. Maier, Unidirectional light scattering with high efficiency at optical frequencies based on low-loss dielectric nanoantennas, *Nanoscale* 8(29), 14184 (2016)
20. C. Wu, N. Arju, G. Kelp, J. A. Fan, J. Dominguez, E. Gonzales, E. Tutuc, I. Brener, and G. Shvets, Spectrally selective chiral silicon metasurfaces based on infrared Fano resonances, *Nat. Commun.* 5, 3892 (2014)
21. B. Hopkins, D. S. Filonov, A. E. Miroshnichenko, F. Monticone, A. Alù, and Y. S. Kivshar, Interplay of magnetic responses in all-dielectric oligomers to realize magnetic Fano resonances, *ACS Photon.* 2, 724 (2015)
22. Z. J. Yang, Fano interference of electromagnetic modes in subwavelength dielectric nanocrosses, *J. Phys. Chem. C* 120(38), 21843 (2016)
23. D. J. Cai, Y. H. Huang, W. J. Wang, W. B. Ji, J. D. Chen, Z. H. Chen, and S. D. Liu, Fano resonances generated in a single dielectric homogeneous nanoparticle with high structural symmetry, *J. Phys. Chem. C* 119(8), 4252 (2015)
24. D. R. Abujetas, M. A. G. Mandujano, E. R. Méndez, and J. A. Sánchez-Gil, High-contrast Fano resonances in single semiconductor nanorods, *ACS Photon.* 4, 1814 (2017)

25. W. Liu, A. E. Miroshnichenko, D. N. Neshev, and Y. S. Kivshar, Broadband unidirectional scattering by magneto-electric core–shell nanoparticles, *ACS Nano* 6(6), 5489 (2012)
26. H. Wang, P. Liu, Y. Ke, Y. Su, L. Zhang, N. Xu, S. Deng, and H. Chen, Janus magneto–electric nanosphere dimers exhibiting unidirectional visible light scattering and strong electromagnetic field enhancement, *ACS Nano* 9(1), 436 (2015)
27. R. Guo, E. Rusak, I. Staude, J. Dominguez, M. Decker, C. Rockstuhl, I. Brener, D. N. Neshev, and Y. S. Kivshar, Multipolar coupling in hybrid metal-dielectric metasurfaces, *ACS Photon.* 3, 349 (2016)
28. H. Chen, L. Shao, Y. C. Man, C. Zhao, J. Wang, and B. Yang, Fano resonance in (gold core)-(dielectric shell) nanostructures without symmetry breaking, *Small* 8(10), 1503 (2012)
29. Z. J. Yang, Q. Q. Wang, and H. Q. Lin, Tunable two types of Fano resonances in metal–dielectric core–shell nanoparticle clusters, *Appl. Phys. Lett.* 103(11), 111115 (2013)
30. M. F. Limonov, M. V. Rybin, A. N. Poddubny, and Y. S. Kivshar, Fano resonances in photonics, *Nat. Photonics* 11(9), 543 (2017)
31. H. Wang, Y. Ke, N. Xu, R. Zhan, Z. Zheng, J. Wen, J. Yan, P. Liu, J. Chen, J. She, Y. Zhang, F. Liu, H. Chen, and S. Deng, Resonance coupling in silicon nanosphere–J-aggregate heterostructures, *Nano Lett.* 16(11), 6886 (2016)
32. J. Wen, H. Wang, W. Wang, Z. Deng, C. Zhuang, Y. Zhang, F. Liu, J. She, J. Chen, H. Chen, S. Deng, and N. Xu, Room-temperature strong light–matter interaction with active control in single plasmonic nanorod coupled with two-dimensional atomic crystals, *Nano Lett.* 17(8), 4689 (2017)
33. E. D. Palik, Handbook of Optical Constants of Solids, Vol. 3, Academic Press, 1998
34. C. F. Bohren and D. R. Huffman, Absorption and Scattering of Light by Small Particles, John Wiley & Sons, 2008
35. A. García-Etxarri, R. Gómez-Medina, L. S. Froufe-Pérez, C. López, L. Chantada, F. Scheffold, J. Aizpurua, M. Nieto-Vesperinas, and J. J. Sáenz, Strong magnetic response of submicron Silicon particles in the infrared, *Opt. Express* 19(6), 4815 (2011)
36. G. Bachelier, I. Russier-Antoine, E. Benichou, C. Jonin, N. Del Fatti, F. Vallee, and P. F. Brevet, Fano profiles induced by near-field coupling in heterogeneous dimers of gold and silver nanoparticles, *Phys. Rev. Lett.* 101(19), 197401 (2008)